Available online at www.sciencedirect.com
SCIENCE DIRECT®
International Journal of Thermal Sciences 45 (2006) 51–59
International Journal of Thermal Sciences
www.elsevier.com/locate/ijts

Entropy generation in a binary gas mixture in the presence of thermal and solutal mixed convection

Kiari Goni Boulama [a], Nicolas Galanis [a,*], Jamel Orfi [b]

[a] *THERMAUS, Génie Mécanique, Université de Sherbrooke, Sherbrooke, QC, J1K 2R1, Canada*
[b] *LESTE, École Nationale d'Ingénieurs de Monastir, Monastir 5019, Tunisia*

Received 15 December 2004; received in revised form 25 April 2005; accepted 25 April 2005

Available online 2 June 2005

Abstract

Steady-state, laminar, fully-developed mixed convection of a binary non-reacting gas mixture flowing upwards in a vertical parallel-plate channel has been investigated from the point of view of the second law of thermodynamics. Analytical expressions are derived for the entropy generation rate for two combinations of boundary conditions: uniform wall temperature with uniform wall concentration (UWT-UWC) and uniform wall heat flux with uniform wall concentration (UHF-UWC). These expressions include three sources of irreversibility: heat conduction, fluid friction and species diffusion. In the UWT-UWC case, the entropy generation rate depends on the thermal and solutal boundary conditions and the mean velocity while in the UHF-UWC case it also depends on the streamwise coordinate. For humid air, the contribution of fluid friction is negligible for both cases while heat conduction and species diffusion effects appear to be of comparable orders of magnitude.

Keywords: Heat transfer; Mass transfer; Mixed convection; Internal flow; Second law of thermodynamics; Analytical solution

1. Introduction

Confined flows with simultaneous heat and mass transfer are of great interest for engineers and scientists since such flows are encountered in a variety of natural phenomena as well as in numerous industrial applications. The physics governing these problems is well understood and interesting experimental, numerical and analytical results have been published for the development of the velocity, temperature and concentration fields. Furthermore, momentum, heat and mass transfer rates have been calculated for some usual geometrical configurations [1].

On the other hand, efficient use of energy is nowadays one of the primary concerns when designing a thermodynamic system. This involves a proper identification and control of entropy generation sources. Hence, the motivation for the second-law analysis in engineering thermal science, the basics of which are outlined in an important paper by Bejan [2].

Local entropy generation in flows with heat transfer and no mass transfer has been investigated for some typical geometries. Thus, Bejan [3] examined the cases of forced thermal convection along a heated plate, across a single cylinder, and inside circular and rectangular ducts. Two sources of irreversibility were identified: thermal conduction and viscous friction. The relative importance of these two effects was found to depend on a dimensionless parameter that combines the Prandtl and Eckert numbers as well as the dimensionless temperature difference between the two walls. Furthermore, a technique for the choice of channel sizes minimizing irreversibility has been proposed.

Similarly, Sahin [4] considered the forced convection laminar flow of a viscous fluid in isothermally heated ducts of different cross-sectional geometries and compared the pumping energy requirements as well as the entropy generation. The author established that circular ducts gener-

* Corresponding author. Tel.: +1 819 821 7144; fax: +1 819 821 7163.
E-mail address: nicolas.galanis@usherbrooke.ca (N. Galanis).

1290-0729/$ – see front matter © 2005 Elsevier SAS. All rights reserved.
doi:10.1016/j.ijthermalsci.2005.04.008

Nomenclature

Br	Brinkman number as defined by Eq. (8) (UWT-UWC case) or Eq. (16) (UHF-UWC case)
C_p	specific heat at constant pressure . $\mathrm{J{\cdot}kg^{-1}{\cdot}K^{-1}}$
$D_{v,a}$	mass diffusivity ..... $\mathrm{m^2{\cdot}s^{-1}}$
D_h	hydraulic diameter ..... m
g	gravitational acceleration ..... $\mathrm{m{\cdot}s^{-2}}$
Gr_T	thermal Grashof number, $= g\beta_T \Delta T D_h^3/\nu^2$
Gr_M	solutal Grashof number, $= g\beta_M(\omega_2-\omega_1)D_h^3/\nu^2$
K_i	rate of formation/extinction of species i ..... $\mathrm{kg{\cdot}m^{-3}{\cdot}s^{-1}}$
M_i	molecular weight for species i ..... $\mathrm{kg{\cdot}mol^{-1}}$
n_i	number density of species i ..... $\mathrm{mol{\cdot}m^{-3}}$
p	static pressure ..... Pa
P	dimensionless pressure, $= (p+\rho g x)/\rho u_0^2$
Pe	Péclet number, $= \rho u_0 D_h C_p/\lambda$
Pr_i	modified Prandtl number for species i as defined by Eq. (9)
Re	Reynolds number, $= u_0 D_h/\nu$
q	externally imposed wall heat flux, conductive heat flux ..... $\mathrm{W{\cdot}m^{-2}}$
q_R	radiative heat flux ..... $\mathrm{W{\cdot}m^{-2}}$
R	universal gas constant ..... $\mathrm{J{\cdot}mol^{-1}{\cdot}K^{-1}}$
R_i	specific gas constant for species i . $\mathrm{J{\cdot}kg^{-1}{\cdot}K^{-1}}$
Sc	Schmidt number $= \nu/D_{v,a}$
S_g	entropy generation rate ..... $\mathrm{W{\cdot}m^{-3}{\cdot}K^{-1}}$
S_g^*	integral entropy production rate as defined by Eq. (17)
T	temperature ..... K
u, v	axial and transverse components of velocity vector ..... $\mathrm{m{\cdot}s^{-1}}$
U, V	dimensionless components of velocity vector $U = u/u_0$ and $V = vD_h/\nu$
$\vec{V}$	diffusion velocity for species i ..... $\mathrm{m{\cdot}s^{-1}}$
W	dimensionless mass fraction of diffusing species, $= (\omega-\omega_1)/(\omega_2-\omega_1)$
X_i	density of body force exerting on species i ..... $\mathrm{N{\cdot}mol^{-1}}$
x, y	axial and transverse coordinates ..... m
X, Y	dimensionless axial and transverse coordinates $X = x/(D_h Re)$ and $Y = y/D_h$

Greek letters

β_M	solutal expansion coefficient
β_T	thermal expansion coefficient ..... $\mathrm{K^{-1}}$
ΔT	temperature difference ($\Delta T = T_2 - T_1$ for UWT or $\Delta T = q_2 D_h/\lambda$ for UHF)
θ	dimensionless temperature $= (T-T_1)/\Delta T$
λ	thermal conductivity ..... $\mathrm{W{\cdot}m^{-1}{\cdot}K^{-1}}$
μ	dynamic viscosity ..... $\mathrm{kg{\cdot}m^{-1}{\cdot}s^{-1}}$
μ_i	chemical potential (partial molar Gibbs energy) for species i ..... $\mathrm{J{\cdot}mol^{-1}}$
ν	kinematic viscosity ..... $\mathrm{m^2{\cdot}s^{-1}}$
ξ	dimensionless parameter, $= \left[\frac{Gr_T}{2Re}\left(1+\frac{q_1}{q_2}\right)\right]^{1/4}$
σ	stress tensor ..... $\mathrm{kg{\cdot}m^{-1}{\cdot}s^{-2}}$
ρ	density ..... $\mathrm{kg{\cdot}m^{-3}}$
Φ	viscous dissipation of energy ..... $\mathrm{W{\cdot}m^{-3}}$
ω	concentration of diffusing species ... (kg of species B)·(kg of mixture)$^{-1}$

Subscripts

0	mean value
1	value on cold wall ($Y = 0$)
2	value on hot wall ($Y = 0.5$)

Abbreviations

UHF	uniform wall heat flux
UWC	uniform wall concentration
UWT	uniform wall temperature

ally lead to the minimum exergetic losses particularly when the frictional contribution to the irreversibility is important.

Demirel [5] investigated the Couette flow of highly viscous fluids between two isothermal cylinders or plates in the presence of positive and negative pressure gradients from the point of view of the second-law of thermodynamics. The well-known fully-developed velocity and temperature profiles were introduced in the expressions for the entropy generation rate, which were afterwards plotted for different Brinkman numbers, angular velocities (circular Couette flow) and pressure gradients (plane Couette flow). Furthermore, the variations of the ratio between the contribution of fluid friction and that of heat conduction to the overall entropy generation rate (or, equivalently, the Bejan number) were presented and discussed.

More recently, Mahmud and Fraser [6] extended the preceding study to fully-developed forced convection plane as well as circular Couette and Poiseuille flows of Newtonian and power-law fluids. In all these configurations, expressions are derived for the entropy generation rates from the known velocity and temperature profiles. However, this study is based on a very restrictive hypothesis: in the general expression for the entropy generation rate, temperature was assumed constant whenever it appears alone (not in a derivative).

Narusawa [7] examined the entropy production in a three-dimensional horizontal and rectangular channel with two adiabatic sidewalls and isothermally heated top and bottom walls. Unlike the previous authors, he took account of the buoyancy forces arising from temperature non-uniformities as well as the subsequent influences on the flow-field solu-

tion. Analytically (for the fully-developed flow region) and numerically (for the developing flow region) derived cross-sectional entropy production rates were then presented and the contributions of heat conduction and viscous dissipation qualitatively and quantitatively analyzed.

When heat transfer and mass transfer occur simultaneously, the thermodynamics of irreversible processes [8] indicate that entropy generation will result from a greater number of sources including chemical reactions, non-uniformity in body forces and chemical potentials, etc. Starting from the relation established by Hirschfelder et al. [8], San et al. [9] obtained an expression for the entropy generation rate in a fully-developed rectangular-duct flow of a binary non reactive gas mixture. According to these authors, the sources of irreversibility are, in this case, the following four: viscous dissipation, heat conduction, mass diffusion and a coupling between the heat and mass transfer processes.

Later on however, Carrington and Sun [10] proved that the fourth and last term (coupling between heat and mass transfer processes) in the entropy generation expression used by San et al. [9] is non-zero only when the thermo-diffusion (Sorét) and diffusion-thermo (Dufour) effects are included in the model.

The present study deals with the fully-developed, laminar, time-independent, mixed convection heat and mass transfer of a binary non-reacting gas mixture flowing upwards between two vertical parallel plates. The channel walls are subjected to asymmetrical uniform temperatures (UWT) or heat fluxes (UHF) and asymmetrical uniform concentrations (UWC). Thus, both temperature and concentration differences exist and yield buoyancy forces. The hydrodynamic, thermal and solutal fields have been derived analytically and published in a previous article by the present authors [11]. The objective here is to investigate the nature and the relative importance of the different sources of irreversibility for such flows. This is the first such evaluation of entropy production for mixed convection in the presence of simultaneous heat and mass transfer.

2. Analysis

The problem under consideration consists of a bi-dimensional flow of a mixture of two non-reacting gases (large amounts of species A and small amounts of species B) between two parallel vertical plates. See Fig. 1. The non-dimensional axial coordinate is X, nil at the bottom where flow enters the channel and increasingly positive upwards, while the dimensionless transverse coordinate is Y with $Y = 0$ at the left wall (hereafter referred to as wall 1) and $Y = 0.5$ at the right wall (hereafter referred to as wall 2). Temperature and mass fraction gradients are imposed across the channel leading to thermal and species diffusion superimposed to the axial transport. On the other hand, buoyancy forces arise from the density differences subsequent to temperature and composition non-uniformity. The governing mass, momentum, energy and species conservation equations were simplified [11] under the following hypotheses:

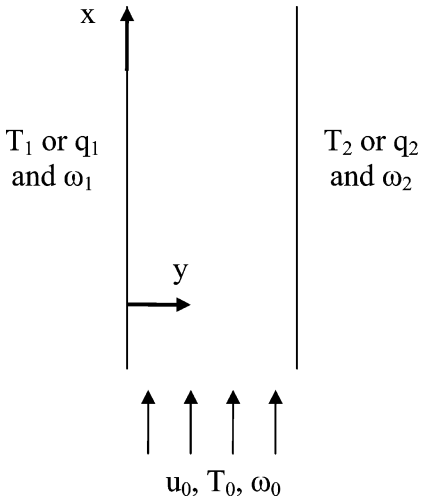

Fig. 1. Schematic representation of the system under study.

- Steady-state laminar flow;
- Boussinesq's hypotheses (all thermophysical properties are constant except for density in the body forces of the momentum conservation equations);
- Viscous dissipation, enthalpy inter-diffusion and pressure work are negligible in the energy conservation equation;
- Species diffusion due to temperature gradients (Sorét effect) and heat diffusion due to species concentration gradients (Dufour effect) are negligible;
- Finally, only the fully-developed region is considered.

Under these conditions, the dimensionless axial velocity, temperature and mass fraction profiles have been derived analytically by the present authors [11]. It has been specifically shown that when the thermal and solutal boundary conditions are both of Dirichlet type (UWT and UWC respectively), the solution depends on a single parameter, the combined buoyancy parameter which is the ratio of the sum of the thermal and the solutal Grashof numbers over the Reynolds number. However, when the thermal boundary conditions are changed to UHF (Newman type boundary conditions), the solution is a function of three parameters: the ratio of the thermal Grashof number to the Reynolds number, the ratio of the solutal Grashof number to the Reynolds number as well as the ratio between the imposed two wall heat fluxes.

The general entropy generation rate derived by Hirschfelder et al. [8] from the energy conservation equation and Maxwell's relation between entropy and internal energy is as follows:

$$S_g = -\frac{1}{T^2}\left[(\vec{q}+\vec{q}_R)\cdot\nabla T\right] - \frac{1}{T}\sigma:\nabla\vec{V} - \sum_i n_i\left[\vec{\overline{V}}_i\cdot\nabla\left(\frac{\mu_i}{T}\right)\right] + \sum_i n_i\left[\vec{\overline{V}}_i\cdot\frac{\vec{X}_i}{T}\right] - \frac{1}{T}\sum_i \mu_i K_i \quad (1)$$

The first term in this expression corresponds to entropy generation caused by heat transfer; the second term is due to viscous dissipation while the third one results from flow non-uniformities (chemical potential and temperature gradients). Entropy generation due to the differences between the body forces exerted on the individual species and that due to chemical reactions constitute the last two terms. Obviously in most common situations several of the preceding effects can be ignored and the expression for the entropy generation rate simplified. In particular, for non-reacting flows and a non-radiating fluid, when the only external body forces are due to gravity and the only non-uniformities leading to chemical potentials are due to temperature and composition differences, it has been proven [10] that this expression can be reduced to:

$$S_g = \frac{\lambda}{T^2}(\nabla T)^2 + \frac{\Phi}{T} + \rho D_{v,a}\overline{R}\sum_i \frac{(\nabla\omega_i)^2}{M_i\omega_i} \quad (2)$$

In the following, the velocity, mass fraction and temperature profiles obtained for the fully-developed flow region [11] are utilized to calculate the entropy generation rate according to Eq. (2) and to evaluate the relative importance of the different contributions. It is recalled that the third term on the right-hand side of Eq. (2) is absent in the works by Bejan [3], Sahin [4], Demirel [5], Mahmud and Fraser [6] as well as Narusawa [7]. Furthermore, the last two studies assumed that the temperature appearing in the denominators of the first two terms on the right-hand side of Eq. (2) is a constant. The validity of this hypothesis is questionable, especially in the presence of a steep yet constant temperature gradient across the channel, as may be the case for fully-developed flows between isothermally heated plates.

3. Walls with uniform temperatures and uniform concentrations (UWT-UWC)

When the channel walls are subjected to asymmetrical uniform temperatures and concentrations, the fully-developed dimensionless velocity, mass fraction and temperature profiles are [11]:

$$U(Y) = \frac{Gr_T + Gr_M}{Re}\left(-\frac{Y^3}{3}+\frac{Y^2}{4}-\frac{Y}{24}\right) - 24Y^2 + 12Y \quad (3)$$

$$W(Y) = 2Y \quad (4)$$

$$\theta(Y) = 2Y \quad (5)$$

All axial derivatives in Eq. (2) are therefore nil and

$$S_g = \frac{\lambda}{T^2}\left(\frac{\mathrm{d}T}{\mathrm{d}y}\right)^2 + \frac{\mu}{T}\left(\frac{\mathrm{d}u}{\mathrm{d}y}\right)^2 + \rho D_{v,a}\overline{R}\left(\frac{1}{M_v\omega}+\frac{1}{M_a(1-\omega)}\right)\left(\frac{\mathrm{d}\omega}{\mathrm{d}y}\right)^2 \quad (6)$$

or, in a dimensionless form

$$\frac{S_g D_h^2}{\lambda} = \left(\theta+\frac{T_1}{\Delta T}\right)^{-2}\left(\frac{\mathrm{d}\theta}{\mathrm{d}Y}\right)^2 + Br\left(\theta+\frac{T_1}{\Delta T}\right)^{-1}\left(\frac{\mathrm{d}U}{\mathrm{d}Y}\right)^2 + \left(\frac{Pr_v}{\omega_1+(\Delta\omega)W}+\frac{Pr_a}{1-(\omega_1+(\Delta\omega)W)}\right)\times\frac{(\Delta\omega)^2}{Sc}\left(\frac{\mathrm{d}W}{\mathrm{d}Y}\right)^2 \quad (7)$$

where Br is the Brinkman number:

$$Br = \frac{\mu u_0^2}{\lambda\Delta T} \quad (8)$$

and Pr_i is a modified Prandtl number defined as:

$$Pr_i = \frac{\mu R_i}{\lambda} \quad (9)$$

With the known analytical expressions of the velocity, temperature and mass fraction profiles, this dimensionless entropy generation rate can be calculated and plotted as a function of the transversal coordinate Y. It is recalled that for the considered combination of boundary conditions, the fully-developed flow solution is independent of the axial coordinate X.

According to Eqs. (3)–(5), the entropy generation rate profile (Eq. (7)) is a function of the combined buoyancy parameter $(Gr_T + Gr_M)/Re$, the Brinkman number Br, the dimensionless temperature difference $\Delta T/T_1$ and the two wall concentrations ω_1 and ω_2. Alternatively, the entropy generation rate profile (Eq. (7)) is a function of the two thermal boundary conditions (T_1 and T_2), the two solutal boundary conditions (ω_1 and ω_2) and the mean velocity (u_0) when assuming a constant geometry and for a given mixture.

4. Walls with uniform heat fluxes and concentrations (UHF-UWC)

When the channel walls are subjected to asymmetrical uniform heat fluxes and concentrations, the fully-developed velocity, mass fraction and temperature profiles are [11]:

$$U(Y) = C_1\exp(\xi Y)\cos(\xi Y) + C_2\exp(-\xi Y)\cos(\xi Y) + C_3\exp(\xi Y)\sin(\xi Y) + C_4\exp(-\xi Y)\sin(\xi Y) \quad (10)$$

$$W(Y) = 2Y \quad (11)$$

$$\theta = \frac{Re}{Gr_T}\left\{2\xi^2(C_3-C_4) - 2\frac{Gr_M}{Re}Y + \xi^2\left[4C_1\cosh(\xi Y)\sin(\xi Y)2C_3\exp(\xi Y)\cos(\xi Y) + 2C_4\exp(-\xi Y)\cos(\xi Y)\right]\right\} \quad (12)$$

The expression for the parameter ξ is specified in the nomenclature while the integration constants C_1, C_2, C_3 and C_4 are calculated by applying the boundary conditions at $Y = 0$ and $Y = 0.5$. It is important to note that for this configuration, the axial variation of the local fluid temperature is not zero. It is given by:

$$\frac{\partial T}{\partial x} = \frac{2(q_1 + q_2)}{\rho C_p u_0 D_h} \tag{13}$$

The entropy generation rate is therefore expressed by:

$$S_g = \frac{\lambda}{T^2}\left(\left(\frac{\partial T}{\partial x}\right)^2 + \left(\frac{\partial T}{\partial y}\right)^2\right) + \frac{\mu}{T}\left(\frac{\mathrm{d}u}{\mathrm{d}y}\right)^2 + \rho D_{v,a}\overline{R}\left(\frac{1}{M_v\omega}\left(\frac{\mathrm{d}\omega}{\mathrm{d}y}\right)^2 + \frac{1}{M_a(1-\omega)}\left(\frac{\mathrm{d}\omega}{\mathrm{d}y}\right)^2\right) \tag{14}$$

or, in a dimensionless form

$$S_g\left(\frac{D_h^2}{\lambda}\right) = \left[\frac{2}{Pe}\left(\frac{q_1}{q_2} + 1\right)\left(\theta + T_1\frac{\lambda}{q_2 D_h}\right)^{-1}\right]^2 + \left(\theta + T_1\frac{\lambda}{q_2 D_h}\right)^{-2}\left(\frac{\partial\theta}{\partial Y}\right)^2 + Br\left(\theta + T_1\frac{\lambda}{q_2 D_h}\right)^{-1}\left(\frac{\mathrm{d}U}{\mathrm{d}Y}\right)^2 + \left(\frac{Pr_v}{\omega_1 + (\Delta\omega)W} + \frac{Pr_a}{1 - (\omega_1 + (\Delta\omega)W)}\right) \times \frac{(\Delta\omega)^2}{Sc}\left(\frac{\mathrm{d}W}{\mathrm{d}Y}\right)^2 \tag{15}$$

where the Brinkman number is here defined as

$$Br = \frac{\mu u_0^2}{q_2 D_h} \tag{16}$$

Eq. (15) and the known analytical expressions of the velocity, mass fraction and temperature profiles (Eqs. (10)–(12) respectively) make it possible to calculate and obtain a graphical representation of the entropy generation rate as a function of the cross-flow position Y. In this case, and according to Eqs. (10)–(12) and (15), the dimensionless entropy generation rate profile is a function of the thermal (q_1 and q_2) and solutal (ω_1 and ω_2) boundary conditions, the mean velocity (u_0) and the local wall temperature T_1 (or, equivalently, the streamwise location X in the channel).

5. Results and discussion

All the following results have been calculated for air and water vapour mixtures, with $Pr_v = 0.32$, $Pr_a = 0.20$ and $Sc = 0.53$.

5.1. Walls with uniform temperatures and uniform concentrations (UWT-UWC)

First, the local entropy generation rate (Eq. (7)) is evaluated for the case of a channel subjected to asymmetrical first kind thermal and solutal boundary conditions (UWT and UWC respectively). For this application, the following conditions are considered: channel hydraulic diameter $D_h = 0.02$ m, mean axial velocity $u_0 = 0.1$ m·s^{-1}, thermal boundary conditions $T_1 = 283$ K and $T_2 = 313$ K and solutal boundary conditions $\omega_1 = 0.004$ and $\omega_2 = 0.034$. For this combination of boundary conditions, the combined buoyancy parameter is $(Gr_T + Gr_M)/Re = 310$, that is, greater than the flow reversal criterion established by the authors in a previous paper [11]. The velocity profile (see Fig. 2) is therefore distorted with very low (and locally negative) values near the cooler wall (at $Y = 0$) and much greater values in the vicinity of the hotter wall (at $Y = 0.5$). Both temperature and mass fraction profiles are linear. These profiles are not reproduced here.

Fig. 3 shows the profile of the dimensionless entropy generation rate due to heat conduction (I), fluid friction (II) and

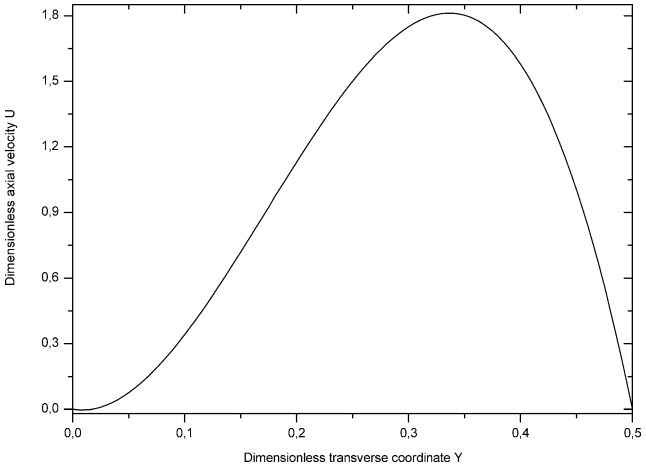

Fig. 2. Dimensionless velocity profile (UWT-UWC case).

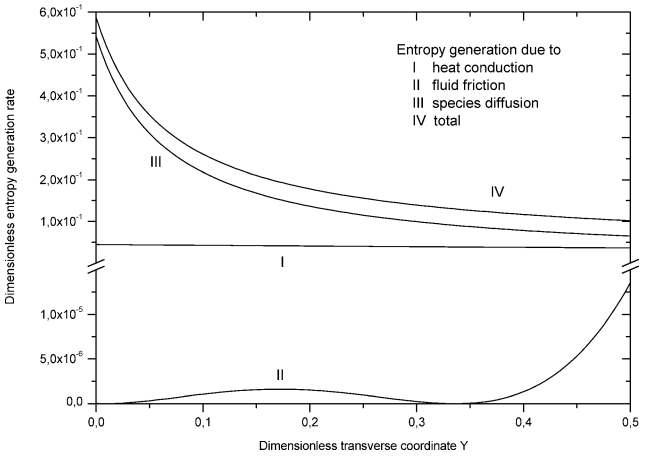

Fig. 3. Dimensionless entropy generation rate profiles (UWT-UWC case).

species diffusion (III) corresponding respectively to the first, second and third terms on the right-hand side of Eq. (7). The first contribution exhibits decreasing values as Y increases from the cooler wall towards the hotter wall. Despite appearances, this profile is not linear but hyperbolic ($\approx Y^{-2}$) consistently with its analytical expression (Eq. (7)) noting that temperature varies linearly with the transverse coordinate Y and, consequently, its derivative is constant.

The shape of the entropy generation rate due to fluid friction across the channel is not easily predictable by simple inspection of the analytical expression (Eq. (7)) because the latter includes a fractional polynomial. On the other hand, the numerically obtained profile of entropy generation due to fluid friction (curve II of Fig. 3) exhibits three local extrema which are definitely related to the minimum, the inflexion point (increasing slope on the left and decreasing slope on the right) and the maximum of the velocity profile (see Fig. 2).

The profile of the dimensionless entropy generation rate due to species diffusion (III) is clearly hyperbolic. This could be predicted from the analytical expression (Eq. (7)) noting that, similarly to the temperature, the water vapour mass fraction varies linearly with Y and, consequently, its derivative is constant throughout the channel.

As far as the quantitative values are concerned, the main observation is that the contribution of fluid friction to the total entropy generation is negligible. On the other hand, species diffusion constitutes the main source of irreversibility and dictates the form of the total entropy generation rate profile.

It is very important to note that all previous results are valid only for water vapour—dry air mixtures and for the combination of the five (T_1, T_2, ω_1, ω_2 and u_0) controlling parameters considered. For any other combination of these parameters or for different mixtures the velocity, temperature and mass fraction profiles must be calculated (according to Eqs. (3)–(5)) and the entropy generation rate re-evaluated (according to Eq. (7)).

As a second step of the analysis, Eq. (7) can be integrated across the channel (from $Y = 0$ to $Y = 0.5$) to obtain the non-dimensional integral entropy production rate:

$$S_g^* = \int_{Y=0}^{Y=0.5} \frac{S_g D_h^2}{\lambda} \mathrm{d}Y \tag{17}$$

The resulting expression is extremely long and is not reproduced in this text for concision. For the present case (isothermal walls with uniform concentrations), this quantity depends on the external parameters T_1, T_2, ω_1, ω_2 and u_0 and is independent of the axial coordinate X.

The effects of the temperature difference ΔT on the integral entropy production rate have been evaluated for $T_1 = 283$ K, $\omega_1 = 0.004$ and $\omega_2 = 0.014$. Thus, the results of Table 1 show that the integral entropy production rate due to heat conduction increases monotonically as the wall-to-wall temperature difference is increased. This could be deduced from Eq. (7) where the increase of ΔT reduces the denominator of the first term on the right-hand side. The same argument applies for the integral entropy production rate due to fluid friction (second term on the right-hand side of Eq. (7)) where, in addition, the increase of ΔT involves a more and more distorted velocity profile and, thus increases the numerator. On the other hand, the water vapour mass fraction is not influenced by the thermal boundary conditions (see Eq. (4)) and the integral entropy production rate due to species diffusion (third term on the right-hand side of Eq. (7)) remains unchanged. It is finally worth noting that the contribution of heat conduction, which is secondary for $\Delta T = 10$ K becomes the predominant effect for $\Delta T = 30$ K.

The effects of the concentration difference $\Delta\omega = \omega_2 - \omega_1$ on the integral entropy production rates have been evaluated for $\omega_1 = 0.004$, $T_1 = 283$ K and $T_2 = 313$ K. From Table 2, the first thing to be noted is that the integral entropy production rate due to heat conduction remains unchanged when the solutal boundary conditions are modified consistently with the temperature profile (Eq. (5)) and the analytical expression of the entropy generation rate (see specifically the first

Table 1
Effects of wall temperature difference on the integral entropy production rates (UWT-UWC case)

	$\Delta T = 10$ K	$\Delta T = 15$ K	$\Delta T = 20$ K	$\Delta T = 25$ K	$\Delta T = 30$ K
Heat conduction	0.0024	0.0053	0.0093	0.0143	0.0203
Fluid friction	6.11×10^{-7}	6.58×10^{-7}	6.98×10^{-7}	7.61×10^{-7}	8.38×10^{-7}
Species diffusion	0.0151	0.0151	0.0151	0.0151	0.0151
Total	0.0175	0.0205	0.0245	0.0295	0.0354

Table 2
Effects of wall concentration difference on the integral entropy production rates (UWT-UWC case)

	$\Delta\omega = 0.000$	$\Delta\omega = 0.010$	$\Delta\omega = 0.015$	$\Delta\omega = 0.020$	$\Delta\omega = 0.030$
Heat conduction	0.0203	0.0203	0.0203	0.0203	0.0203
Fluid friction	8.05×10^{-7}	8.38×10^{-7}	8.56×10^{-7}	8.73×10^{-7}	9.11×10^{-7}
Species diffusion	0.0000	0.0151	0.0283	0.0434	0.0778
Total	0.0203	0.0354	0.0486	0.0637	0.0981

term on the right-hand side of Eq. (7)). As a further result, the denominator of the second term on the right of Eq. (7) is unchanged and the slight variation in the integral entropy production rate due to fluid friction is a consequence of the extra distortion of the velocity profile with increasing $\Delta\omega$. On the other hand, the integral entropy production rate due to species diffusion grows rapidly from zero when $\Delta\omega$ is nil and becomes, for higher values of $\Delta\omega$, the most important contribution to the overall irreversibility source.

The combinations of the results in these two tables indicate that using small driving potentials ΔT and $\Delta\omega$ reduces thermodynamic irreversibility. However, for a more complete optimization of the process other variables (geometry, mass flow rate, etc.) should also be considered.

5.2. Walls with uniform heat fluxes and concentrations (UHF-UWC)

In this section, Eq. (15) is used to calculate the local entropy generation rate and the relative importance of the different contributions for the case of a channel subjected to asymmetrical second kind thermal boundary conditions and first kind solutal boundary conditions (UHF and UWC respectively). The same fluid mixture and geometrical configuration as in the preceding section are considered. The mean axial velocity is $u_0 = 0.1\ \mathrm{m{\cdot}s^{-1}}$, the solutal boundary conditions are $\omega_1 = 0.004$ and $\omega_2 = 0.034$ and the thermal boundary conditions are $q_1 = -75\ \mathrm{W{\cdot}m^{-2}}$ and $q_2 = 150\ \mathrm{W{\cdot}m^{-2}}$. Finally, as indicated earlier, the local temperature of wall 1 appears explicitly in Eq. (15) and is therefore a parameter to take into account. Here, we consider that we are in the fully-developed flow region at the streamwise position where $T_1 = 283$ K.

The velocity and temperature profiles are calculated from Eqs. (10) and (12) and are shown in Fig. 4. The water vapour mass fraction profile is linear (Eq. (11)) and is therefore not plotted in this text. The temperature profile (Eq. (12)), unlike in the UWT-UWC case (Eq. (5)), is no longer linear and its slope varies continuously across the channel. Accordingly, the behaviour of the entropy generation due to heat conduction (sum of the first two terms on the right-hand side of Eq. (15)) is not easily predictable. In fact, curve I of Fig. 5 reveals that this quantity passes through a minimum value near the cool wall ($Y = 0$), maintains a positive slope in the major part of the channel, reaches a maximum close to the warm wall ($Y = 0.5$) and then decreases.

The entropy generation rate due to fluid friction (curve II of Fig. 5) exhibits a fairly similar qualitative and quantitative shape as the one for the UWT-UWC case (see Fig. 3). One just has to note that the first local extremum vanishes because the flow does not reverse direction for the combination of controlling parameters under consideration. The second (corresponding to the inflexion point) and third (maximum of velocity profile) extrema however still remain.

Finally, the entropy generation rate due to species diffusion (III) is not affected by the temperature nor the velocity profiles (see Eq. (11)). It displays exactly the same form as for the UWT-UWC case, that is, it decreases hyperbolically with increasing Y. However, in contrast to the UWT-UWC

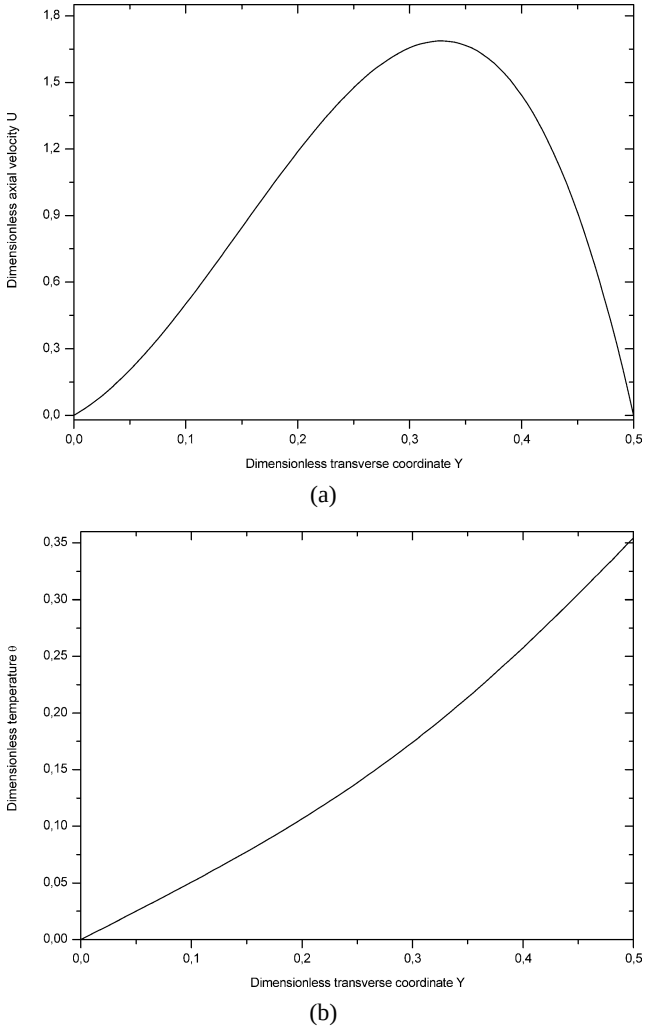

Fig. 4. (a) Dimensionless velocity profile (UHF-UWC case). (b) Dimensionless temperature profile (UHF-UWC case).

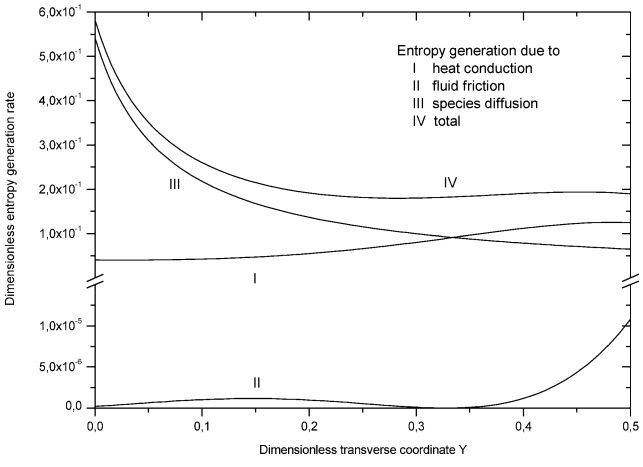

Fig. 5. Dimensionless entropy generation rate profiles (UHF-UWC case).

Table 3
Effects of wall heat flux ratio on the integral entropy production rates (UHF-UWC case)

	$q_1/q_2 = -0.75$	$q_1/q_2 = -0.5$	$q_1/q_2 = 0$	$q_1/q_2 = 0.5$	$q_1/q_2 = 1$
Heat conduction	0.0225	0.0169	0.0106	0.0106	0.0166
Fluid friction	6.30×10^{-7}	6.10×10^{-7}	5.83×10^{-7}	5.72×10^{-7}	5.75×10^{-7}
Species diffusion	0.0289	0.0289	0.0289	0.0289	0.0289
Total	0.0514	0.0458	0.0395	0.0395	0.0455

Table 4
Effects of wall concentration difference on the integral entropy production rates (UHF-UWC case)

	$\Delta\omega = 0.000$	$\Delta\omega = 0.010$	$\Delta\omega = 0.015$	$\Delta\omega = 0.020$	$\Delta\omega = 0.025$
Heat conduction	0.0226	0.0223	0.0222	0.0221	0.0219
Fluid friction	5.93×10^{-7}	6.07×10^{-7}	6.14×10^{-7}	6.23×10^{-7}	6.31×10^{-7}
Species diffusion	0.000	0.0151	0.0282	0.0434	0.0600
Total	0.0226	0.0375	0.0504	0.0654	0.0819

case (and for the combination of controlling parameters considered in Fig. 3) where this term constituted the main contribution to the total entropy generation throughout the channel, in the present case the contribution of heat conduction becomes predominant for the greater values of the transverse coordinate Y. The two terms I and III are of the same order of magnitude and concurrently govern the evolution of the total entropy generation rate.

Once again, these results should not be generalized. Instead, for any particular combination of boundary conditions and/or mixture materials, Eqs. (10)–(12) must be re-evaluated for the velocity, temperature and concentration profiles. Then Eq. (15) must be applied to calculate the entropy generation rates attributable to heat conduction, fluid friction and species diffusion respectively.

In the following paragraph the effects of the ratio between the externally imposed wall heat fluxes and those of the wall concentration differences on the integral entropy production rate are investigated. It is to be noted that, because an explicit analytical primitive does not exist for Eq. (15), a numerical integration via Simpson's rule has been carried out from $Y = 0$ to $Y = 0.5$ to obtain the value of the integral entropy production rate. The results are presented in Tables 3 and 4.

In order to produce Table 3, the left wall (at $Y = 0$) has been subjected to various heat fluxes without changing the other parameters ($u_0 = 0.1$ m·s^{-1}, $q_2 = 100$ W·m^{-2}, $\omega_1 = 0.001$, $\omega_2 = 0.011$ and $T_1 = 293$ K). The first conclusion arising from this table is that the integral entropy production due to heat conduction is important when the left wall is substantially cooled, decreases when the ratio between the two wall heat fluxes increases, reaches a minimum and finally increases. Integral entropy production due to fluid friction follows a similar tendency. The minimum value may correspond in this case to the least distorted velocity profile (least sharp slopes). As in the UWT-UWC case, this term is several orders of magnitude smaller than the other terms. Finally, since the term corresponding to species diffusion is independent of the thermal boundary conditions (see Eqs. (11) and (15)), the effects of q_1/q_2 on the total integral entropy production rate reduce to those on the integral entropy production rate due to heat conduction. The minimum total entropy production rate corresponds to a value of q_1/q_2 between 0 and 0.5. This indicates that in order to reduce thermodynamic irreversibilities it is recommended, for the conditions considered here, to heat the flow from both walls so that the ratio of the heat fluxes lies in this interval.

Table 4 finally summarizes the effects of the wall concentration difference $\Delta\omega$ on the integral entropy production rates. The reported results have been obtained for $q_1 = 0$, $q_2 = 150$ W·m^{-2}, $\omega_1 = 0.004$ and at the axial position where $T_1 = 293$ K. Table 4 reveals that, unlike for the UWT-UWC case (Dirichlet type thermal and solutal boundary conditions), the entropy production due to heat conduction is slightly influenced by the solutal boundary conditions. This is expected because for the UHF-UWC case (Newman type thermal boundary conditions superimposed to Dirichlet type solutal boundary conditions), the temperature profile (Eq. (12)) contains the solutal Grashof number. In fact, Table 4 indicates that the integral entropy production rate due to heat conduction diminishes monotonically as the wall concentration difference increases. On the other hand, when $\Delta\omega$ (or, equivalently, Gr_M) increases, the velocity profile becomes more distorted. As a consequence, the integral entropy production rate due to fluid friction increases. The variation of the integral entropy production rate due to species diffusion is the same as that described previously for the UWT-UWC case. The combination of these three tendencies results in a monotonic increase of the total with $\Delta\omega$.

The comments on process optimization formulated at the end of the preceding section apply also in the present case.

6. Conclusion

Analytical expressions for the entropy generation rate in the presence of fully-developed, laminar and time-independent simultaneous thermal and solutal mixed convection in a vertical channel have been derived for the first time based on

the analytical flow field solution obtained in a previous article by the same authors [11]. Three sources of irreversibility have been identified: heat conduction, fluid friction and species diffusion. For all the situations under consideration, the entropy generation rate due to fluid friction is shown to be negligible. This result is consistent with the earlier analysis by Bejan [3]. However, heat conduction and species diffusion effects are always of comparable order of magnitude and concurrently determine the shape of the total entropy generation rate profile. This profile is influenced by both thermal and solutal boundary conditions as well as by the mean axial velocity when asymmetrical uniform temperatures and concentrations are imposed to the channel walls (UWT-UWC configuration). However, when second kind thermal boundary conditions are considered (UHF-UWC configuration), the entropy generation rate profile also depends on the streamwise location in the channel.

The integral entropy production rates have been calculated for different combinations of the controlling parameters and the subsequent variations of the individual contributions have been appraised. For the case of water vapour and dry air mixtures, it has been shown that the contribution of fluid friction is negligible while the total may exhibit a minimum with respect to q_1/q_2 or increase monotonically with respect to ΔT and $\Delta\omega$.

Acknowledgements

The financial support of this work by the Natural Sciences and Engineering Research Council of Canada is gratefully acknowledged. The first author also wishes to thank Professor Yves Mercadier of the University of Sherbrooke for his precious advices.

References

[1] A. Ali Cherif, A. Daïf, Étude numérique du transfert de chaleur et de masse entre deux plaques planes verticales en présence d'un film liquide ruisselant sur l'une des plaques chauffées, Int. J. Heat Mass Transfer 42 (13) (1999) 2399–2418.

[2] A. Bejan, Second-law analysis in heat transfer and thermal design, Adv. Heat Transfer 15 (1982) 1–58.

[3] A. Bejan, A study of entropy generation in fundamental convective heat transfer, ASME Trans. J. Heat Transfer 101 (1979) 718–725.

[4] A.Z. Sahin, A second-law comparison for optimum shape of duct subjected to constant wall temperature and laminar flow, Heat Mass Transfer 33 (5–6) (1998) 425–430.

[5] Y. Demirel, Thermodynamic analysis of thermomechanical coupling in Couette flow, Int. J. Heat Mass Transfer 43 (22) (2000) 4205–4212.

[6] S. Mahmud, R.A. Fraser, The second-law analysis in fundamental heat transfer problems, Int. J. Thermal Sci. 42 (2) (2003) 177–186.

[7] U. Narusawa, The second-law analysis of mixed convection in rectangular ducts, Heat Mass Transfer 37 (2–3) (2001) 197–203.

[8] J.O. Hirschfelder, C.F. Curtiss, R.B. Bird, Molecular Theory of Gases and Liquids, Wiley, New York, 1954 (Chapter 11).

[9] J.Y. San, W.M. Worek, Z. Lavan, Entropy generation in combined heat and mass transfer, Int. J. Heat Mass Transfer 30 (7) (1987) 1359–1369.

[10] C.G. Carrington, Z.F. Sun, Second law analysis of combined heat and mass transfer phenomena, Int. J. Heat Mass Transfer 34 (11) (1991) 2767–2773.

[11] K. Boulama, N. Galanis, Analytical solution for fully developed mixed convection between parallel vertical plates with heat and mass transfer, ASME Trans. J. Heat Transfer 126 (3) (2004) 381–388.